
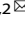


ARTICLE



Bilirubin represents a negative regulator of ILC2 in allergic airway inflammation

Juan He^{1,2,8}, Guanmin Jiang^{3,8}, Xing Li^{4,8}, Qiang Xiao^{2,3}, Yingying Chen^{1,2}, Haixu Xu², Gaoyu Liu^{1,2}, Aihua Lei¹, Pan Zhou², Kun Shi⁵, Quan Yang⁶, Meng Zhao⁷, Zhi Yao²  and Jie Zhou^{1,2} 

© The Author(s), under exclusive licence to Society for Mucosal Immunology 2021

Group 2 innate lymphoid cells (ILC2s) play an important role in allergic airway inflammation. Despite recent advances in defining molecular mechanisms that control ILC2 development and function, the role of endogenous metabolites in the regulation of ILC2s remains poorly understood. Herein, we demonstrated that bilirubin, an end product of heme catabolism, was a potent negative regulator of ILC2s. Bilirubin metabolism was found to be significantly induced during airway inflammation in mouse models. The administration of unconjugated bilirubin (UCB) dramatically suppressed ILC2 responses to interleukin (IL)–33 in mice, including cell proliferation and the production of effector cytokines. Furthermore, UCB significantly alleviated ILC2-driven airway inflammation, which was aggravated upon clearance of endogenous UCB. Mechanistic studies showed that the effects of bilirubin on ILC2s were associated with downregulation of ERK phosphorylation and GATA3 expression. Clinically, newborns with hyperbilirubinemia displayed significantly lower levels of ILC2 with impaired function and suppressed ERK signaling. Together, these findings indicate that bilirubin serves as an endogenous suppressor of ILC2s and might have potential therapeutic value in the treatment of allergic airway inflammation.

Mucosal Immunology (2022) 15:314–326; <https://doi.org/10.1038/s41385-021-00460-0>

INTRODUCTION

Group 2 innate lymphoid cells (ILC2s) are type 2 innate immune cells that lack both antigen-specific receptors and pattern recognition receptors. The importance of ILC2s in driving allergic inflammation is well recognized.¹ Upon allergen exposure, lung epithelium-derived cytokines, such as interleukin (IL)–33, IL–25, and thymic stromal lymphopoietin (TSLP), bind to the corresponding ILC2 receptors, which leads to the expansion and activation of ILC2s in the lung.^{1,2} The activated ILC2s then rapidly secrete effector cytokines, which not only initiate allergic inflammation at an early stage but also promote the activation of Th2 responses at a later stage.^{3–5} ILC2s are thus considered a novel biomarker and immunotherapeutic target for airway inflammation in patients with asthma.^{6–8}

In addition to cytokines, which play critical roles in ILC2 responses, some other endogenous mediators, including metabolites, sex hormones, and neural-derived peptides, are emerging as important regulators of ILC2s.^{1,9} The arachidonic acid metabolites leukotrienes and prostaglandins (such as PGD₂) are positive regulators of ILC2s, whereas lipoxin A₄ (LXA₄), prostaglandin E₂ (PGE₂), and prostacyclin (PGI₂) can suppress ILC2 activation.^{10–13} These findings suggest a crucial role for endogenous factors in ILC2 biological function.

Bilirubin is an endogenous end product of heme degradation. The enzyme heme oxygenase (HO) cleaves the heme to produce biliverdin, which is then reduced to unconjugated bilirubin (UCB), and the latter circulates in the blood after binding to albumin. The beneficial effects of bilirubin in suppressing inflammatory disorders have long been appreciated.^{14,15} Thus, patients with jaundice displayed spontaneous remission of inflammatory disorders, including asthma, allergy, and rheumatoid arthritis.^{14,16–18} Furthermore, bilirubin at physiologically concentrations has broad effects on the functions of multiple immune cells.¹⁴ For example, treatment with UCB was reported to dramatically attenuate Th2 responses in a mouse model of asthma,^{19,20} although this conclusion has been disputed in other reports.^{21,22} These studies indicate the importance of UCB during airway inflammation; however, the underlying mechanisms are not fully understood.

Considering the anti-inflammatory effects of bilirubin and the importance of ILC2s in airway inflammation, we attempted to investigate the potential role of bilirubin in the biological function of ILC2s. Administration of UCB dramatically suppressed ILC2 responses, therefore alleviating airway inflammation in mice. In contrast, depletion of endogenous bilirubin production clearly aggravated airway inflammation. Bilirubin responses were

¹Joint Program in Immunology, Department of Internal Medicine, Guangzhou Women and Children's Medical Center, Zhongshan School of Medicine, Sun Yat-sen University, Guangzhou, China. ²Key Laboratory of Immune Microenvironment and Disease (Ministry of Education), Department of Immunology, School of Basic Medical Sciences, Tianjin Medical University, Tianjin, China. ³Department of Clinical Laboratory, The Fifth Affiliated Hospital of Sun Yat-sen University, Zhuhai, China. ⁴The Third Affiliated Hospital of Sun Yat-sen University, Guangzhou, China. ⁵Department of Obstetrics and Gynaecology, Guangzhou Women and Children's Medical Center, Guangzhou, China. ⁶Key Laboratory of Immunology, Sino-French Hoffmann Institute, School of Basic Medical Sciences; Guangdong Provincial Key Laboratory of Allergy & Clinical Immunology, The Second Affiliated Hospital, Guangzhou Medical University, Guangzhou, China. ⁷Department of Clinical Laboratory, Tianjin Medical University Cancer Institute and Hospital, Tianjin, China. ⁸These authors contributed equally: Juan He, Guanmin Jiang, Xing Li. [✉]email: yaozhi@tmu.edu.cn; zhujie@tmu.edu.cn

Received: 11 February 2021 Revised: 29 August 2021 Accepted: 16 September 2021

Published online: 22 October 2021

associated with reduced ERK signaling and GATA3 expression. Notably, newborns with hyperbilirubinemia showed a reduced ILC2 levels with impaired function. This study suggests potential therapeutic value of bilirubin in the treatment of ILC2-driven allergic airway inflammation.

RESULTS

Bilirubin suppresses ILC2 responses to IL-33

To investigate the potential effect of bilirubin on ILC2s, the activity of bilirubin metabolism was evaluated in ILC2-driven airway inflammation models. The concentrations of total bilirubin were markedly elevated in the peripheral blood from papain- or IL-33-treated mice, in which ILC2s plays a major role in driving the airway inflammation (Supplementary Fig. S1A). Meanwhile, the number of red blood cells was also elevated in the papain model (Supplementary Fig. S1B). Immunohistochemical staining further confirmed the accumulation of bilirubin in inflamed lungs compared with that in tissues under steady-state conditions (Supplementary Fig. S1C). Interestingly, the elevation of total bilirubin and the increased red blood cells were also observed in patients with severe asthma compared with those in patients with mild asthma and healthy donors (Supplementary Fig. S1D). Furthermore, the mRNA expression of the key enzymes of bilirubin metabolism, including HO-1 (*Hmox1*), biliverdin reductase B (*Bilvrb*), and UDP-glucuronosyltransferase 1A1 (*Ugt1a1*), was significantly upregulated in inflamed lungs in both papain- and IL-33-challenged animals (Supplementary Figs. S1E and S1F). These findings suggested that local bilirubin metabolism was enhanced during ILC2-driven lung inflammation. This induction was mainly observed in lung epithelial cells (EPCAM⁺ cells), rather than in CD45⁺ immune cells from the lung (Supplementary Fig. S1G). Collectively, these observations indicate that the activity of bilirubin metabolism in lung epithelial cells was induced during airway inflammation.

To directly evaluate the effect of bilirubin on ILC2s, C57BL/6J mice were injected with UCB (intraperitoneal [i.p.], 25 mg/kg daily) after IL-33 administration (i.p., 500 ng/mouse daily). This dosage of UCB was within the physiological range to avoid harmful effects (20–170 μ M)^{23,24} and did not cause any liver damage, as indicated by the activities of aspartate aminotransferase (AST) and alanine aminotransferase (ALT) (Supplementary Fig. S1H). Lung ILC2s were defined as CD45⁺Lin⁻CD90.2⁺CD25⁺ST2⁺GATA3⁺ cells, as described previously (Supplementary Fig. S2A).^{25,26} As expected, IL-33 dramatically induced the expansion of lung ILC2s and enhanced the production of the effector cytokines IL-5 and IL-13 in vehicle-treated mice, which were reduced approximately by half upon coadministration of UCB (Fig. 1a, b). Consistent with the systemic effect of IL-33 on ILC2 responses,²⁵ the frequencies of ILC2s in multiple tissues, including the bone marrow (BM),²⁷ mesenteric lymph node (mLN),²⁵ liver,²⁸ adipose tissue,²⁹ and peripheral blood,³⁰ were dramatically decreased upon coadministration of UCB (Fig. 1c–f). Of note, the function of ILC2s in the mLN and liver was also markedly impaired by UCB (Fig. 1g). In agreement with the impaired ILC2 responses, the proliferation of lung ILC2s was significantly suppressed by UCB (Fig. 1h). However, there was no noticeable induction of apoptosis in ILC2s (Supplementary Fig. S2B). These findings suggest that UCB impairs ILC2 responses to IL-33.

Bilirubin suppresses the function of lung ILC2s

To further investigate the effect of bilirubin on ILC2s, purified lung ILC2s were adoptively transferred into immunodeficient NCG (NOD-Prkdc^{em26Cd52}Il2rg^{em26Cd22}/Nju) mice, which lack T cells, B cells, and ILC2s.²⁵ The mice were then administered with IL-33 (intranasally [i.n.]) and UCB (i.p.) for 3 days, PBS was used as the vehicle control. In the absence of IL-33 stimulation, the levels of ILC2s were comparable in the vehicle and UCB treatment groups, indicating that the migration or survival of ILC2s was not

apparently affected by UCB treatment. The administration of IL-33 dramatically increased the number of ILC2s in the lungs of recipient mice, whereas the coadministration of UCB almost completely abrogated this effect (Fig. 2a). The number of eosinophils (Fig. 2b), as well as the amounts of IL-5 and IL-13 in the bronchoalveolar lavage (BAL) fluid (Fig. 2c), was consequently diminished in the IL-33- and UCB-cotreated recipient mice compared with their number in the IL-33 alone group. The remission of airway inflammation after UCB treatment was further evidenced using hematoxylin and eosin (H&E) staining (Fig. 2d). Further in vitro culture of lung ILC2s showed that UCB suppressed the production of multiple effector cytokines, including IL-5, IL-13, granulocyte-macrophage colony stimulating factor (GM-CSF), IL-6, amphiregulin (Areg), and IL-9, in a concentration-dependent manner (Fig. 2e). All the concentrations used were within the physiological range and were nontoxic to ILC2s (Supplementary Fig. S2C). Meanwhile, different concentrations of bilirubin did not show any noticeable effects on ST2 expression on ILC2s (Supplementary Figs. S2D and S2E), which indicated that bilirubin might diffuse into ILC2s rather than affecting IL-33 receptor expression. Thus, bilirubin negatively regulates the function of ILC2s both in vivo and in vitro.

Bilirubin causes remission of ILC2-driven allergic airway inflammation

As ILC2s are key players in allergic airway inflammation,^{31,32} we next investigated the effect of UCB on ILC2-induced airway inflammation using a model of the intranasal instillation of the protease papain.^{25,26} As expected, the administration of papain caused dramatic infiltration of eosinophils (Fig. 3a) and enhanced type 2 cytokine production (Fig. 3b) in the BAL fluid, whereas the coadministration of UCB significantly diminished these inflammatory responses compared with those in the vehicle controls (Fig. 3a, b). The remission of ILC2-driven lung inflammation, caused by UCB, was further confirmed by H&E staining (Fig. 3c). Of note, the proliferation of lung ILC2s (Fig. 3d), as well as their cell counts and the production of effector cytokines (Fig. 3e, f), was reduced approximately by half upon coadministration of UCB.

To further confirm the previous findings, we employed *Alternaria alternata* (*A. alternata*), a clinically relevant allergen, to induce lung inflammation.²⁵ Consistently, the total number of lung ILC2s (Fig. 3g), their proliferation, and the secretion of effector cytokines (Fig. 3h, i) were clearly diminished upon UCB treatment. As expected, the frequency of eosinophils (Fig. 3j) and the concentrations of IL-5 and IL-13 (Fig. 3k) in the BAL fluid were decreased in UCB-treated mice. The amelioration of lung inflammation was further confirmed by H&E staining (Fig. 3l). These findings indicate that UCB significantly alleviates ILC2-driven airway inflammation.

It has been reported that UCB can suppress Th2 cells in allergic airway inflammation.¹⁹ Using an ovalbumin (OVA)-induced mouse model of lung inflammation, we confirmed that both Th2 and ILC2 responses were impaired in UCB-treated mice (Supplementary Figs. S3A and S3B) when lung inflammation was alleviated (Supplementary Figs. S3C and S3D). Considering the existence of a crosstalk between Th2 cells and ILC2s during allergic inflammation,³³ *Rag-1*^{-/-} mice, which lack T and B cells, were used to induce allergic inflammation. The results showed that the coadministration of UCB markedly decreased type 2 cytokine production (Supplementary Fig. S3E) and eosinophil levels (Supplementary Fig. S3F) in the BAL fluid compared with those in the papain alone group. Moreover, the total number of ILC2s (Supplementary Fig. S3G), their production of effector cytokines (Supplementary Fig. S3H) and ILC2 proliferation (Supplementary Fig. S3I) were consistently decreased in UCB-treated mice. The attenuation of lung inflammation was further evidenced by H&E staining (Supplementary Fig. S3J). Therefore, we concluded that the effect of UCB on ILC2s was independent of T cells.

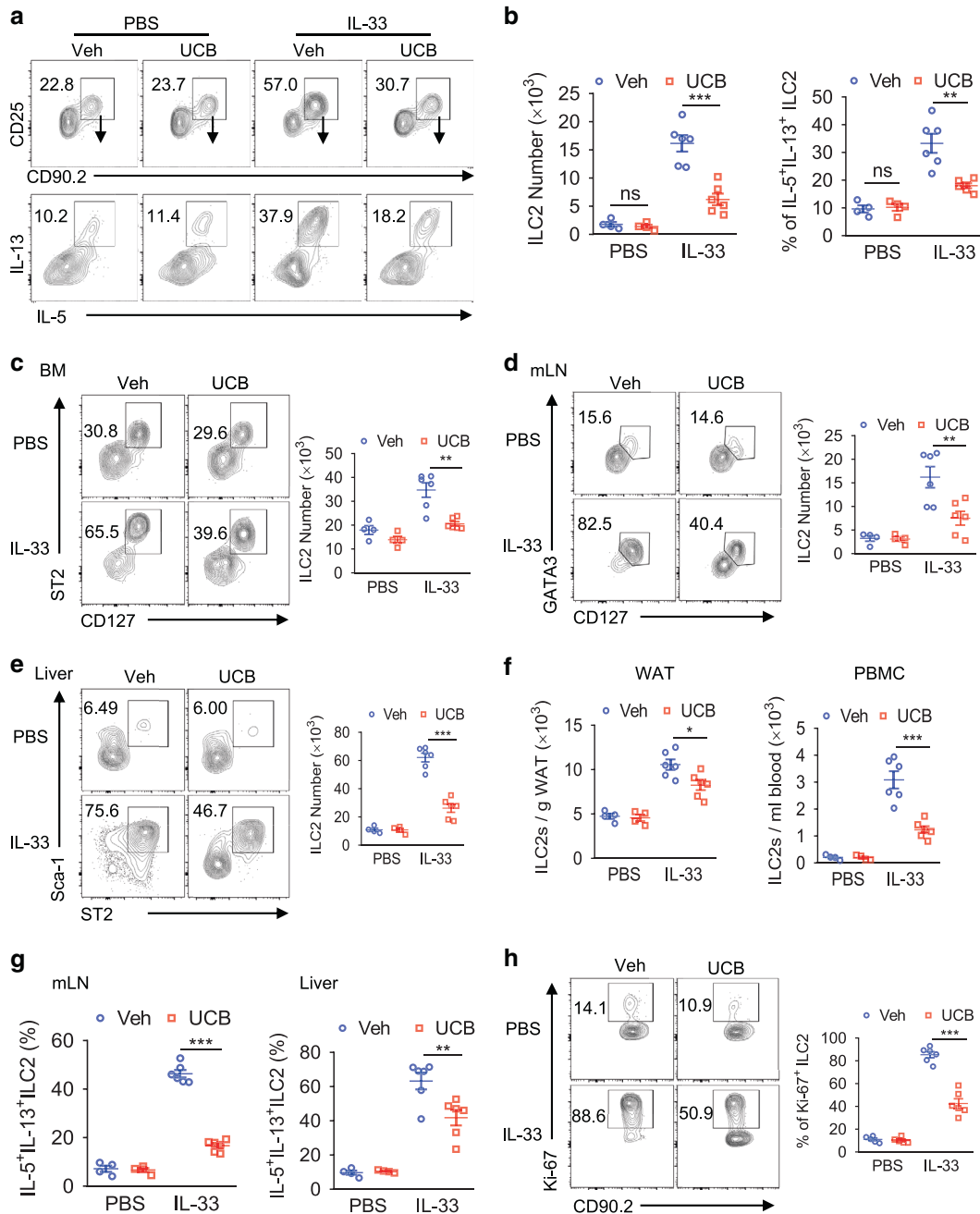


Fig. 1 Bilirubin suppresses ILC2 responses to IL-33. C57BL/6J mice were injected with the vehicle (Veh) or UCB (*i.p.*, 25 mg/kg daily) for 5 days. From day 2 mice were administered with IL-33 (*i.p.*, 500 ng/mouse, daily) or PBS vehicle control for consecutive 4 days ($n = 4-6$ per group). **a, b** Flow cytometric analysis of lung ILC2s and their secretion of IL-5 and IL-13. Both representative results (**a**) and mean \pm SEMs from all mice (**b**) were shown. Flow cytometric analysis of ILC2s in different tissues including (**c**) bone marrow (BM, $CD45^+Lin^-CD90.2^+CD127^+ST2^+$), (**d**) mesenteric lymph node (mLN, $CD45^+Lin^-CD90.2^+CD127^+GATA3^+$), (**e**) Liver ($CD45^+Lin^-C-kit^+CD127^+Sca-1^+ST2^+$), (**f**) WAT (white adipose tissue, WAT) ($CD45^+Lin^-Sca-1^+CD127^+CD25^+$) and peripheral blood mononuclear cells (PBMC, $CD45^+Lin^-CD90.2^+CD127^+ST2^+$). **g** Frequencies of $IL5^+IL13^+$ ILC2s in mLN and liver in mice from **d** and **e**. **h** The proliferation of lung ILC2s was determined by Ki-67 staining. Data are representative of three independent experiments, mean \pm SEMs from all mice were shown. Unpaired Student's *t* test was used. ** $p < 0.01$, *** $p < 0.001$. Numbers within flow plots indicate the percentages of cells gated.

To investigate whether the inhibitory effect of bilirubin is specific to ILC2s, we used a *Citrobacter rodentium* (CR)-induced colitis model to evaluate the effects of UCB on ILC1s and ILC3s. Consistent with previous reports,^{34,35} the administration of UCB attenuated CR-induced colitis, as indicated by a milder decrease in the body weight and a reduced shortening of the colon length (Supplementary Figs. S4A and S4B). Flow cytometric analysis

showed no noticeable differences in the ILC1 levels and their production of IFN- γ (Supplementary Figs. S4C and S4D), as well as in the ILC3 levels and their production of IL-17A, IL-22, and IFN- γ in the colon (Supplementary Figs. S4E and S4F), between the vehicle- and UCB-treated groups. Meanwhile, the frequencies of ILC2s ($CD45^+Lin^-CD90.2^+GATA3^+$) in the colon were also evaluated by flow cytometry. The results showed that UCB did not affect the

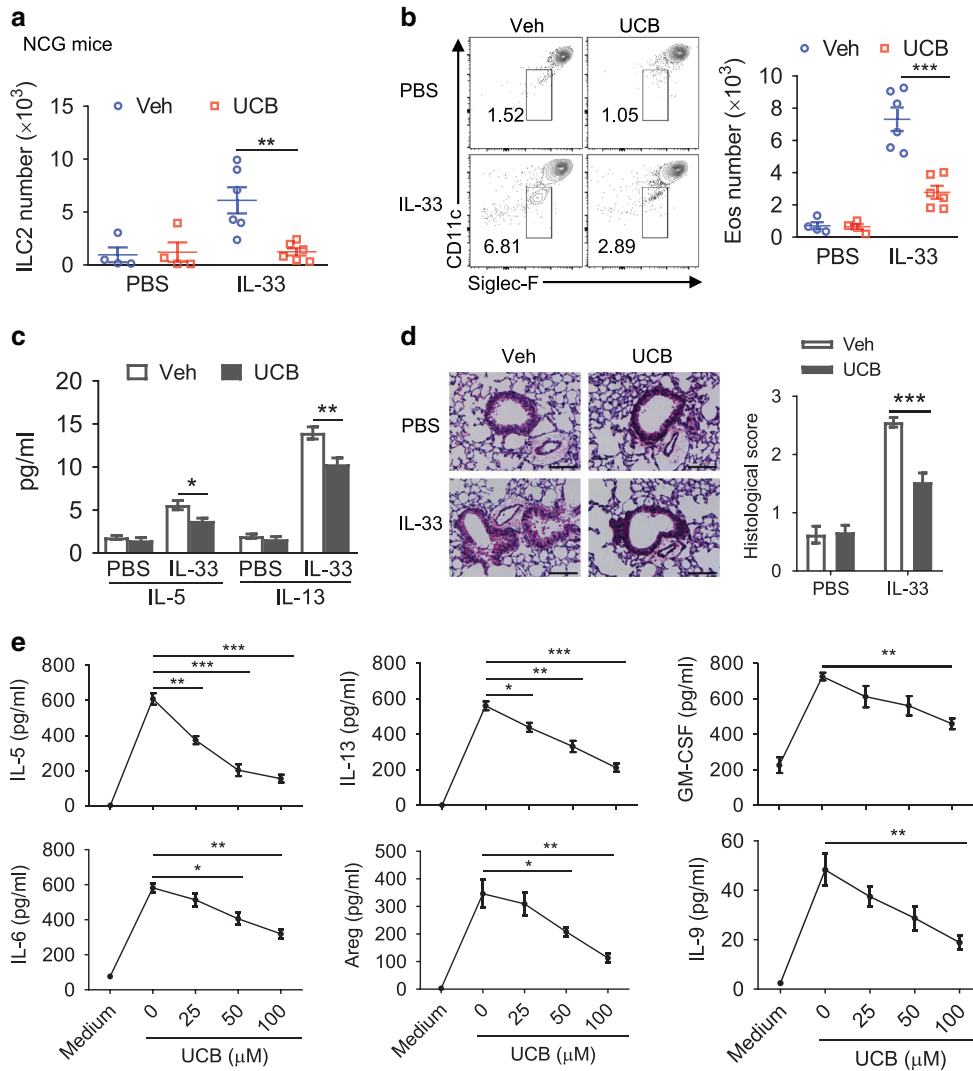


Fig. 2 Bilirubin impairs ILC2 function in response to IL-33 challenge. **a–d** Equal number of lung ILC2s (3×10^4) sorted from IL-33 challenged WT mice were intravenously injected into NCG mice, followed by intranasal administration with IL-33 ($n = 6$ per group) or PBS ($n = 4$ per group) in the presence or absence of UCB (25 mg/kg) treatment for 3 d. **a** The numbers of lung ILC2s in NCG recipients were evaluated by flow cytometry. **b** The frequencies and absolute numbers of eosinophils in BAL were evaluated by flow cytometry. **c** The amounts of IL-5 and IL-13 in BAL were measured by ELISA. **d** Representative H&E staining of lung sections (bars, 100 μ m) and the inflammation was determined by semi-quantitative scoring. **e** Lung ILC2s from mice were cultured for 3 days with IL-2, IL-7 and IL-33 with increasing concentration of UCB, the amounts of effector cytokines in the supernatants were measured by ELISA. Cells cultured in medium containing IL-2 and IL-7 were used as control. Data are representative of three independent experiments, mean \pm SEMs were shown. Unpaired Student's *t* test (**a–c**) or one-way ANOVA with Bonferroni post-test (**e**) were used. * $p < 0.05$, ** $p < 0.01$, *** $p < 0.001$. Numbers within flow plots indicate the percentages of cells gated.

levels of ILC2 in the colon (Supplementary Fig. S4G). It has been reported that the exposure to UCB does not have an effect on Th2 lymphocytes in colitis.³⁴ According to the results to date, intestinal ILC2s and Th2s may not be affected by UCB in colitis. The above results also indicate that UCB may not affect the function of other ILC subsets.

Clearance of endogenous bilirubin aggravates airway inflammation

To further investigate its effect on ILC2s, we depleted endogenous bilirubin during lung inflammation using two different approaches. First, zinc protoporphyrin IX (ZnPP), a specific inhibitor of the HO-1 enzyme, which controls bilirubin production,³⁶ was used in a papain-induced airway inflammation model. As expected, total bilirubin levels were markedly decreased by ZnPP treatment (Fig. 4a). Notably, the administration of ZnPP significantly aggravated the papain-induced airway inflammation, as indicated by the number of

eosinophils and the amounts of the IL-5 and IL-13 cytokines in the BAL fluid (Fig. 4b, c), as well as by H&E staining of lung tissues (Fig. 4d). Meanwhile, ZnPP remarkably enhanced the proliferation of lung ILC2s and facilitated their expansion and the production of effector cytokines (Fig. 4e, f). Considering that HO-1 could also block the production of carbon monoxide, another immunomodulator,³⁷ TCPOBOP, a potent activator of bilirubin clearance,³⁸ was alternatively used to deplete endogenous bilirubin. First, we confirmed that, as expected, the total bilirubin levels were markedly decreased by TCPOBOP treatment (Supplementary Fig. S4H). In line with the results of ZnPP treatment, higher eosinophil infiltration and elevated IL-5 and IL-13 levels in the BAL fluid, as well as aggravated lung inflammation, were observed upon TCPOBOP treatment (Fig. 4g–i). As expected, the total lung ILC2 counts, as well as cytokine production and ILC2 proliferation, were elevated (Fig. 4j, k). These results indicate that the clearance of endogenous bilirubin aggravates allergic airway inflammation.

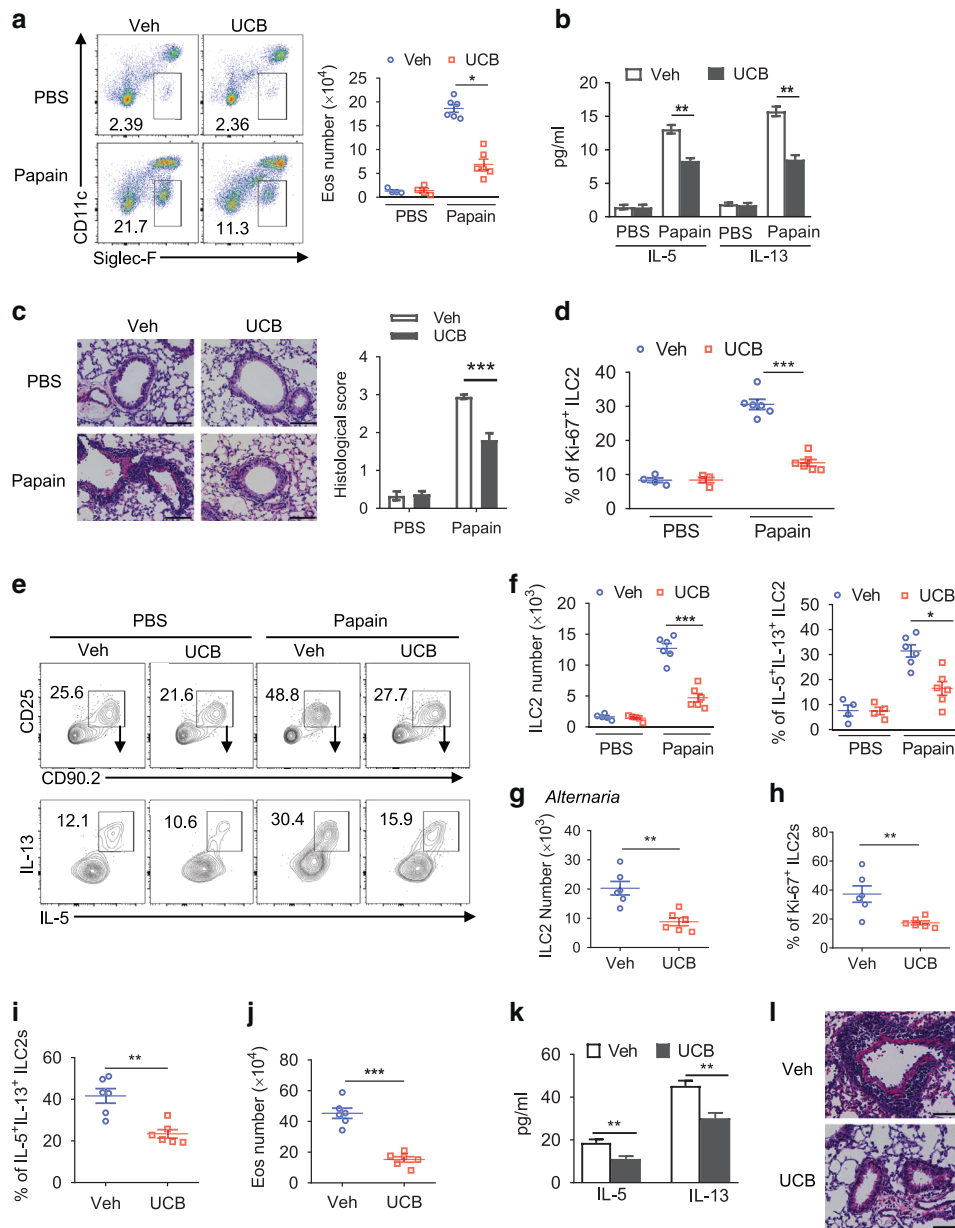


Fig. 3 Bilirubin causes remission of ILC2-driven allergic airway inflammation. **a–f** WT mice were intranasally administered with papain or PBS 6 h after unconjugated bilirubin (UCB) or vehicle (Veh) treatment for consecutive 5 d ($n = 4–6$ per group). Mice were sacrificed 24 h after the last treatment. **a** The frequencies and number of eosinophils in BAL were evaluated by flow cytometry. **b** The amount of IL-5 and IL-13 in BAL was measured by ELISA. **c** Representative H&E staining of lung sections (bars, 100 μ m). **d** The proliferation of lung ILC2s was determined by Ki-67 staining. **e** The frequencies of lung ILC2s and IL-5⁺IL-13⁺ ILC2s were determined by flow cytometry. Cells were stimulated with cocktail for 4 h. **f** The statistical results of **e**. **g–i** WT mice were intranasally challenged with extract of *Alternaria alternata* for 4 d ($n = 6$ per group). Mice were sacrificed 24 h after the last treatment. The number (**g**) and the proliferation (**h**) of lung ILC2s were evaluated by flow cytometry. **i** The frequencies of IL-5⁺IL-13⁺ ILC2s in lungs after cell stimulation cocktail treatment for 4 h. **j** The absolute number of eosinophils in BAL. **k** The amounts of IL-5 and IL-13 in BAL were measured by ELISA. **l** Representative H&E staining of lung sections (bars, 100 μ m). Data are representative of two (**g–i**) to three (**a–f**) independent experiments. Error bars show mean \pm SEM; * $p < 0.05$; ** $p < 0.01$; *** $p < 0.001$ by unpaired Student's *t* test. Numbers within flow plots indicate the percentages of cells gated.

ERK signaling and GATA3 expression are reduced by bilirubin
GATA3 is the master regulator of ILC2s.³⁹ To investigate the mechanisms underlying bilirubin-mediated ILC2 responses, the level of the GATA3 protein was evaluated. Flow cytometric analysis showed that UCB significantly downregulated the levels of GATA3 in mouse lung ILC2s both in the in vivo papain model (Fig. 5a) and in in vitro cell culture (Fig. 5b). Moreover, the mRNA expression levels of *Il5*, *Il13*, *Il2ra*, and *Cdkn2b*, which are known downstream targets of GATA3,⁴⁰ were consistently changed in ILC2s upon UCB treatment (Fig. 5c). No noticeable differences were observed in the *Gata3* mRNA levels

(Fig. 5c), suggesting that the dysregulation of GATA3, caused by UCB, occurs at the posttranscriptional level. The expression of other ILC2 regulators, such as *Ets1*, *Rora*, and *Gfi1*, showed no apparent differences (Fig. 5c). Notably, the overexpression of GATA3 almost completely rescued the defective cytokine production by ILC2s that was caused by UCB (Supplementary Fig. S5A and Fig. 5d).

It is well known that bilirubin inhibits the phosphorylation of a variety of intracellular proteins, including extracellular signal-regulated kinase (ERK)1/2,^{41,42} to exert its biological functions upon diffusion into cells. ERK signaling has been reported to

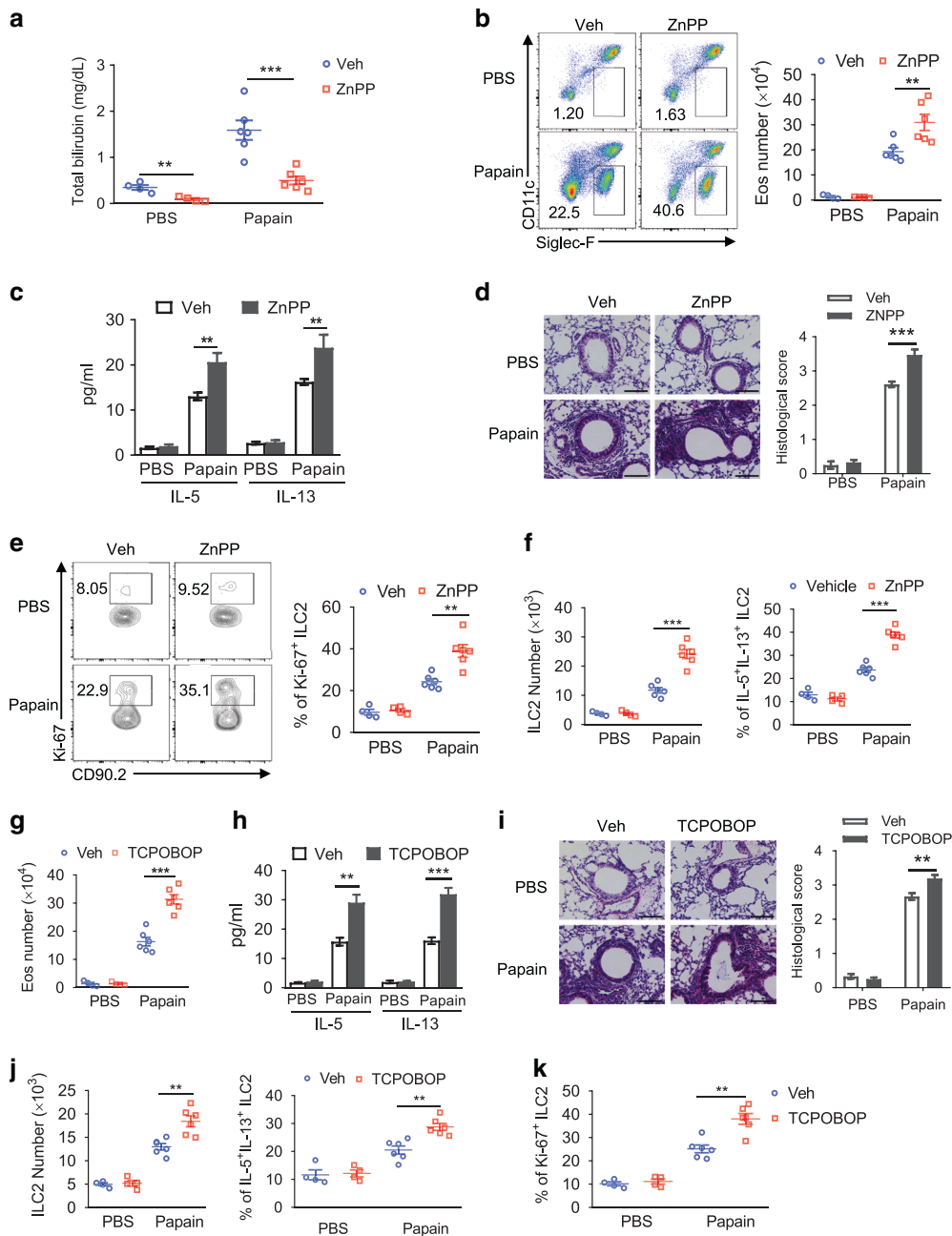


Fig. 4 Clearance of endogenous bilirubin aggravates airway inflammation. **a–f** C57BL/6J mice were intranasally administered with PBS or papain 6 h after vehicle (Veh) or ZnPP (25 mg/kg) treatment for 5 days ($n = 4–6$ for each group). Mice were sacrificed 24 h after the last treatment. **a** Total bilirubin levels in plasma. **b** The frequencies and numbers of eosinophils in BAL were evaluated by flow cytometry. **c** The amounts of IL-5 and IL-13 in BAL were measured by ELISA. **d** Representative H&E staining of lung sections (bars, 100 μ m) and the inflammation was determined by semi-quantitative scoring. **e** The proliferation of lung ILC2s was determined by Ki-67 staining. **f** The numbers of ILC2s and the frequencies of IL-5⁺IL-13⁺ ILC2s in lungs were determined by flow cytometry. **g–k** C57BL/6J mice were intranasally administered with papain or PBS 6 h after vehicle (Veh) or TCPOBOP (3 mg/kg) treatment for 5 days ($n = 4–6$ for each group). Mice were sacrificed 24 h after the last treatment. **g** The numbers of eosinophils in BAL were determined by flow cytometry. **h** The amounts of IL-5 and IL-13 in BAL were measured by ELISA. **i** Representative H&E staining of lung sections (bars, 100 μ m) and the inflammation was determined by semi-quantitative scoring. **j** The absolute numbers of lung ILC2s and the frequencies of IL-5⁺IL-13⁺ ILC2s in lungs were determined by flow cytometry. **k** The proliferation of lung ILC2s were determined by flow cytometry. Data are representative of three independent experiments, mean \pm SEMs were shown. Unpaired Student's *t* test was used. ** $p < 0.01$, *** $p < 0.001$. Numbers within flow plots indicate the percentages of cells gated.

regulate the stability of GATA3 via ubiquitin-mediated degradation⁴³ and also participate in the functional regulation of ILC2s.⁴⁴ ERK signaling was therefore evaluated in UCB-treated ILC2s. The results showed that UCB significantly inhibited ERK phosphorylation (p-ERK1/2) both in vivo and in vitro (Fig. 5e, f). Pretreatment with the ERK agonist honokiol⁴⁵ rescued the effect of UCB on

ILC2s, including the p-ERK1/2 (Fig. 5f) and GATA3 levels (Fig. 5g), cell proliferation (Fig. 5h), and the production of IL-5 and IL-13 (Fig. 5i). It has been reported that PKC, a classic upstream of ERK,^{46,47} is strongly involved in ILC2 function.⁴⁸ Next, we evaluated the expression of PKC in UCB-treated ILC2s and found that UCB significantly reduced PKC phosphorylation (p-PKC) in lung ILC2s

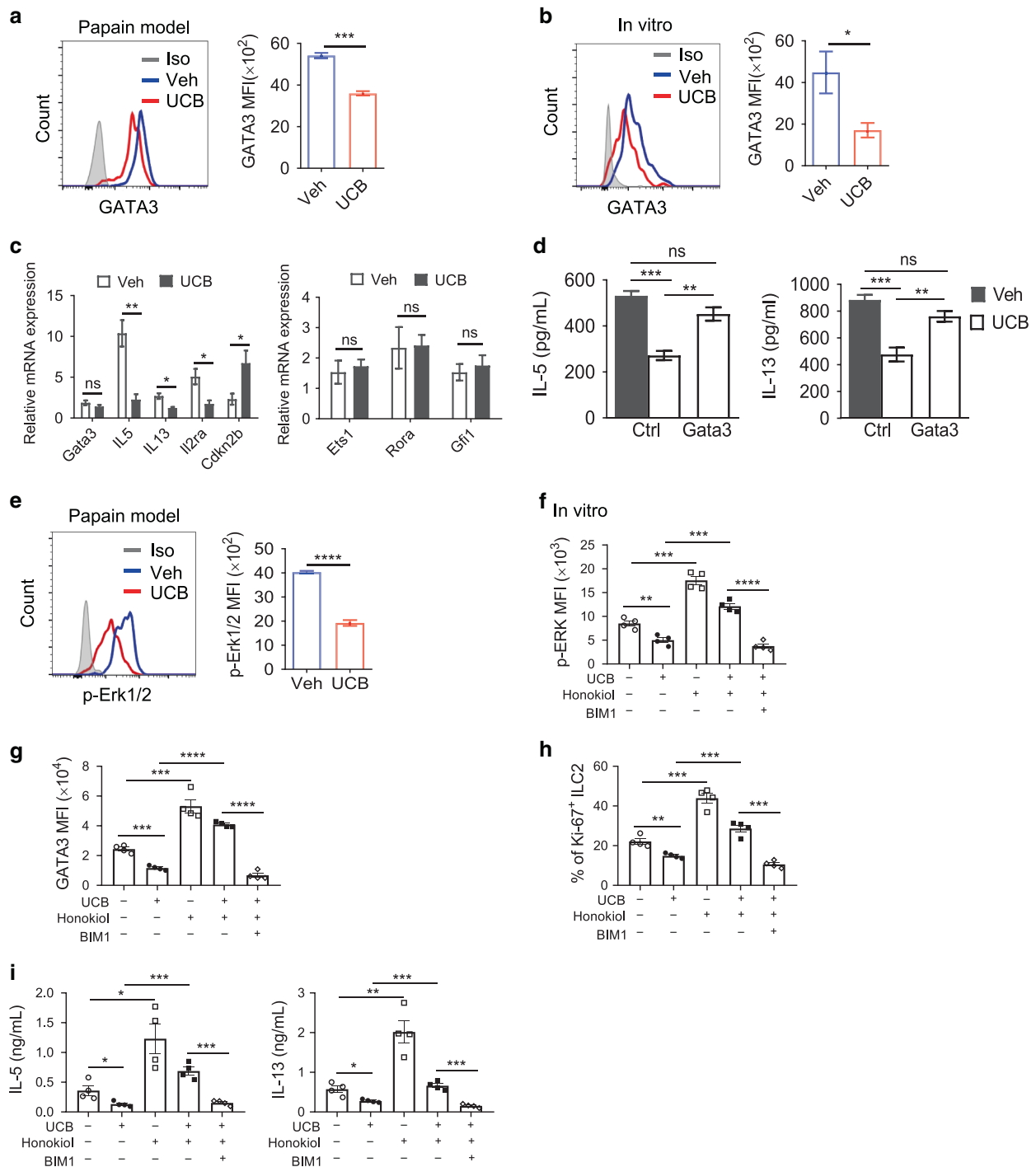


Fig. 5 ERK signaling and GATA3 expression are reduced by bilirubin. **a** Flow cytometric analysis of GATA3 expression in lung ILC2s from mice treated with UCB or vehicle (Veh) upon papain administration ($n = 3$). Both representative results (left) and mean \pm SEMs were shown. MFI mean fluorescence intensity. **b** Flow cytometric analysis of GATA3 expression in sorted lung ILC2s treated with UCB (50 μ M) or Vehicle in the presence of IL-2, IL-7 and IL-33 for 3 days. **c** The mRNA expression of *Gata3*, *Il5*, *Il13*, *Il2ra* and *Cdkn2b* (left), and *Ets1*, *Rora* and *Gfi1* (right) in sorted lung ILC2s. **d** Lung ILC2s were infected with retrovirus expressing GATA3 or empty control, followed by treatment with UCB (50 μ M) or Vehicle in the presence of IL-2, IL-7, IL-33 for 4 days. The amounts of IL-5 and IL-13 in the culture supernatants were measured by ELISA. **e** Flow cytometric analysis of p-ERK1/2 levels in lung ILC2s from mice treated with UCB or PBS vehicle in the papain model ($n = 3$). **f** Lung ILC2s were treated with vehicle or UCB (50 μ M) and/or Honokiol (5 μ M) and/or BIM1 (5 μ M) in the presence of IL-2, IL-7 and IL-33 for 48 h. Flow cytometric analysis of p-ERK1/2 levels was performed. **g** Lung ILC2s were cultured in the presence of IL-2, IL-7, IL-33, with the indicated treatments for 3 days, the level of GATA3 was determined by flow cytometry. **h** The proliferation of lung ILC2s was determined by Ki-67 staining, after culture in the presence of IL-2, IL-7, and IL-33 with indicated treatments for 3 days. **i** The amounts of IL-5 and IL-13 in the supernatants from **g** were measured by ELISA. Data are representative of two (**a**, **d** and **e**) or three (**b**, **c**, and **f**–**i**) independent experiments. Error bars show mean \pm SEM. Data were analyzed by unpaired Student's *t* test (**a**–**f**) or one-way ANOVA with Bonferroni post-test (**g**–**i**). * $p < 0.05$, ** $p < 0.01$, *** $p < 0.001$, **** $p < 0.0001$, ns not significant.

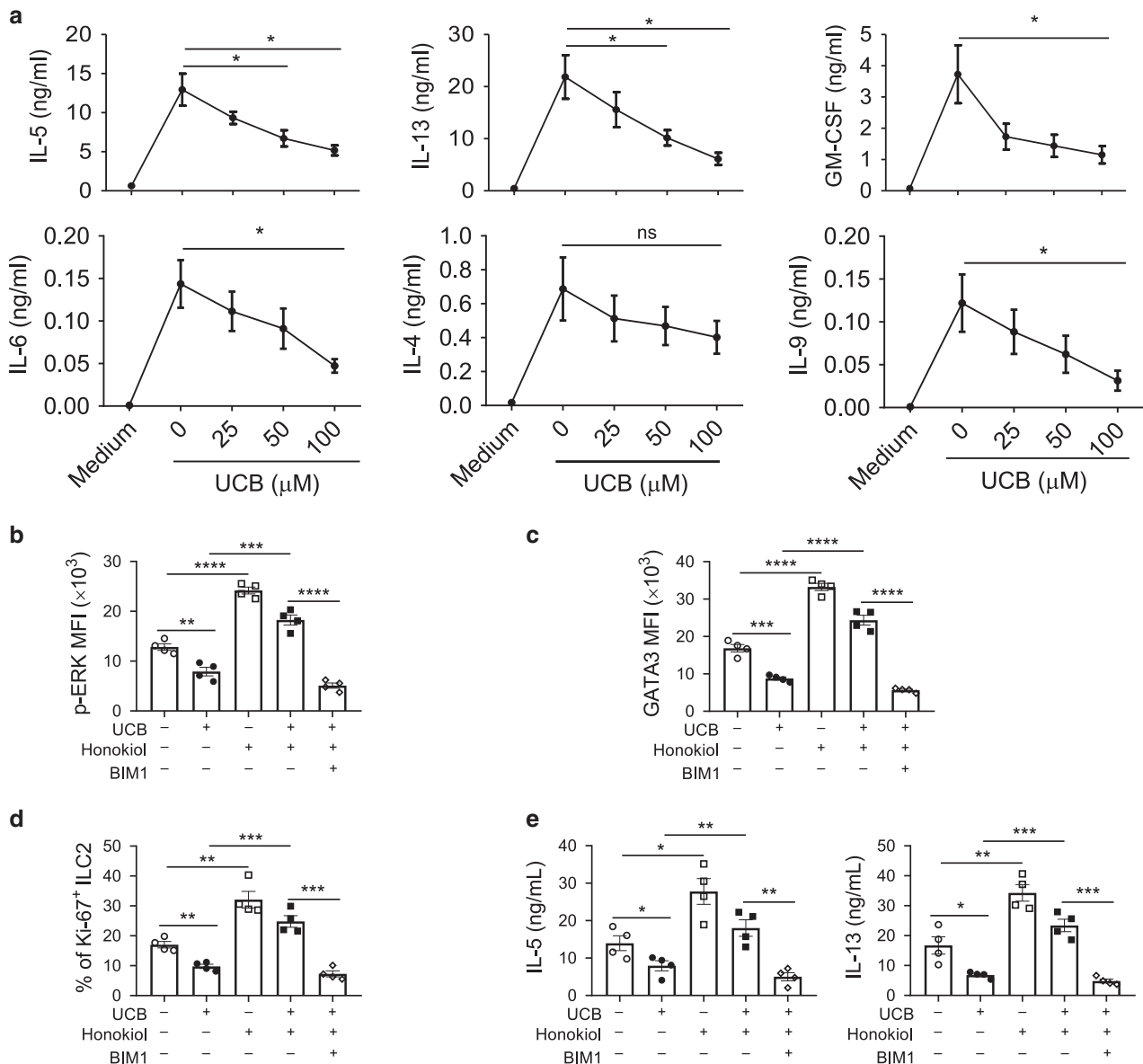


Fig. 6 ERK signaling and GATA3 expression are reduced by bilirubin on human ILC2s. **a** Human ILC2s sorted from cord blood were stimulated for 3 days with IL-2 and IL-7 or IL-2, IL-7 plus IL-33 in the presence of increasing concentrations of UCB. The amounts of indicated cytokines in the supernatants were measured by ELISA. Cells cultured in medium containing IL-2 and IL-7 were used as control. **b** Human ILC2s from cord blood were treated with UCB or vehicle (Veh) and/or Honokiol (5 μM) and/or BIM1 (5 μM) for 48 h. Flow cytometric analysis of p-ERK1/2 levels was performed in sorted human ILC2s. **c** Flow cytometric analysis of GATA3 expression in sorted human ILC2s cultured in the presence of IL-2, IL-7, and IL-33 with the indicated treatments for 3 d. **d** The proliferation of sorted human ILC2s was determined by Ki-67 staining in the presence of IL-2, IL-7, and IL-33 with the indicated treatments for 3 d. **e** The amount of IL-5 and IL-13 in the supernatants from **d** was measured by ELISA. Data are representative of three independent experiments. Error bars show mean ± SEM; * $p < 0.05$; ** $p < 0.01$; *** $p < 0.001$ by unpaired Student's *t* test (**b–e**) or one-way ANOVA with Bonferroni post-test (**a**). ns not significant.

(Supplementary Fig. S5B). The coadministration of the PKC inhibitor bisindolylmaleimide I (BIM I) almost completely abrogated the effects of honokiol on ILC2s (Fig. 5f–i). These results suggest that the effects of bilirubin on ILC2s may be associated with the suppression of PKC-ERK1/2 signaling.

Next, we examined the inhibitory effects of bilirubin on human ILC2s. In line with the observations in mice, UCB significantly suppressed the production of effector cytokines, including IL-5, IL-13, GM-CSF, IL-6, IL-4, and IL-9, by human ILC2s in a concentration-dependent manner (Fig. 6a). Flow cytometric analysis showed that the p-ERK1/2 (Fig. 6b) and GATA3 (Fig. 6c) levels were markedly decreased after UCB treatment of human ILC2s. Honokiol treatment significantly rescued the p-ERK1/2 (Fig. 6b) and GATA3 levels

(Fig. 6c), ILC2 proliferation (Fig. 6d), and their production of IL-5 and IL-13 (Fig. 6e) by UCB-treated ILC2s. Meanwhile, the coadministration of BIM I abrogated these effects (Fig. 6b–e), while ERK agonists did not overcome the blockade of PKC. PKC inhibition by BIM I might reduce the responsiveness of ERK to its agonists in UCB-treated ILC2s. These results suggest that, similarly to our murine studies, in human ILC2s the effects of bilirubin are associated with reduced PKC-ERK1/2 signaling and GATA3 expression.

Newborns with hyperbilirubinemia display reduced ILC2 levels and function

Clinical studies have indicated that newborns with hyperbilirubinemia (HB) have a lower risk of airway inflammation.⁴⁹

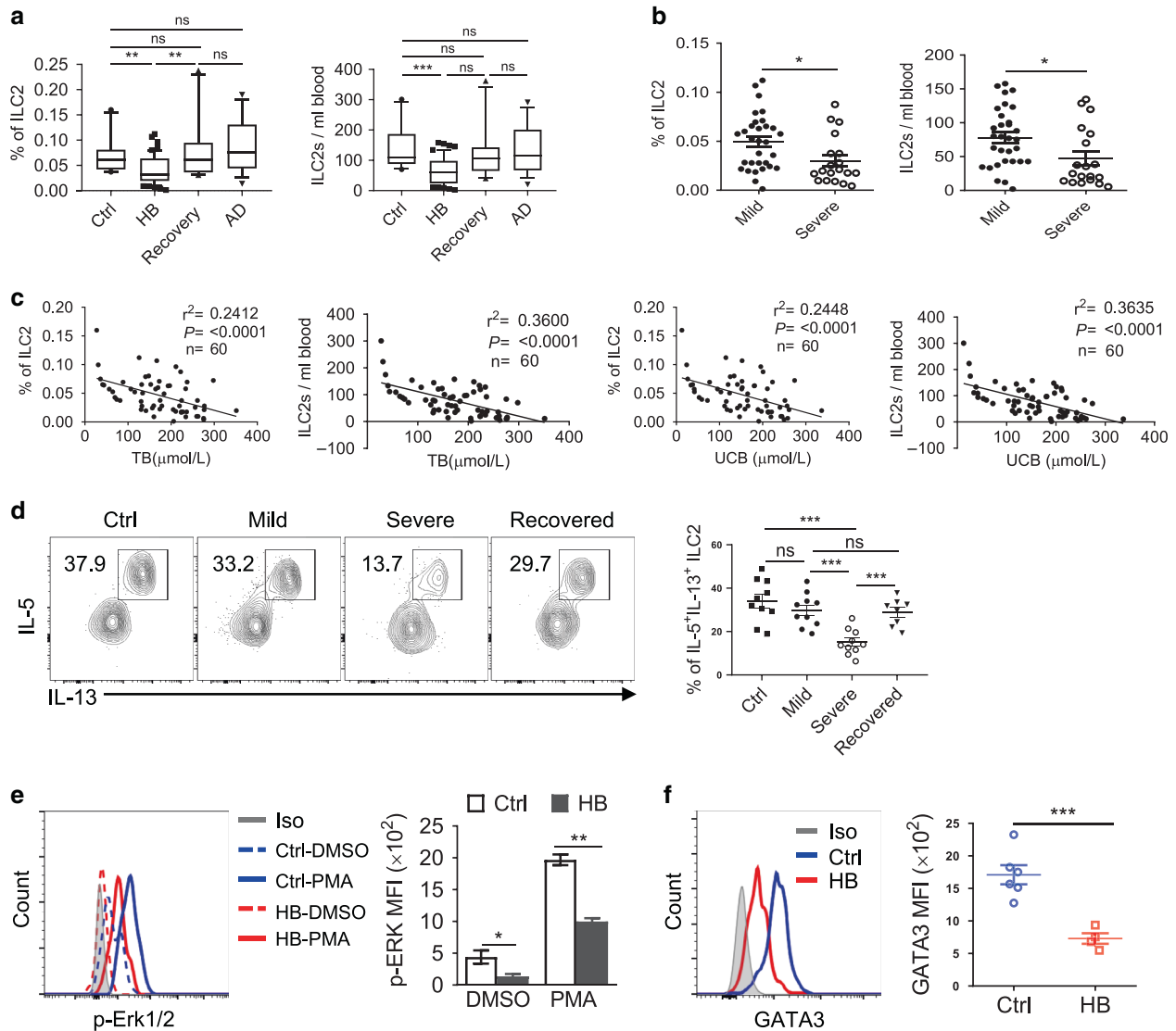


Fig. 7 Newborns with hyperbilirubinemia display lower level of ILC2s with impaired function. **a** The proportions of human ILC2s in PBMC and their absolute cell counts in the peripheral blood were analyzed by flow cytometry, including healthy control infants (Ctrl, $n = 10$), infants with hyperbilirubinemia (HB, $n = 50$), infants recovered from hyperbilirubinemia (Recovery, total bilirubin lower than $85 \mu\text{mol/L}$) ($n = 10$), and healthy adult donors (AD, $n = 19$). **b** The levels of ILC2 in the peripheral blood of infants with hyperbilirubinemia from **a** were analyzed based on the severity of hyperbilirubinemia. Mild: total bilirubin $< 221 \mu\text{mol/L}$ ($n = 31$), severe: total bilirubin $\geq 221 \mu\text{mol/L}$ ($n = 19$). **c** Correlation between the frequencies of ILC2 in the peripheral blood and total bilirubin (TB) or UCB in infants ($n = 60$). **d** Flow cytometric analysis of IL-5⁺IL-13⁺ ILC2s in the peripheral blood from infants with mild ($n = 10$) or severe hyperbilirubinemia ($n = 10$), and infants recovered from hyperbilirubinemia ($n = 8$) and healthy control ($n = 10$). Cells were treated with cytokine stimulation cocktail for 4 h before analysis. **e** Representative flow analysis of p-ERK1/2 levels in ILC2s of PBMCs from healthy (Ctrl) ($n = 5$) and hyperbilirubinemia (HB) newborns ($n = 5$). Cells were stimulated with PMA (a known inducer of p-ERK) or DMSO for 15 min before analysis. **f** Flow cytometric analysis of GATA3 expression in ILC2s of PBMCs from healthy (Ctrl) ($n = 6$) and hyperbilirubinemia (HB) newborns ($n = 4$). Data are representative of three independent experiments. Error bars show mean \pm SEM; Unpaired Student's *t* test was used. * $p < 0.05$, ** $p < 0.01$, *** $p < 0.001$, ns not significant. Correlations were analyzed using Spearman's rank correlation test. Numbers within flow plots indicate the percentages of cells gated.

Considering the negative regulation of ILC2s by UCB, we evaluated whether the levels and function of ILC2s were impaired in newborns with HB. Human ILC2s were gated as CD45⁺Lin⁻CD127⁺CRTH2⁺ (Supplementary Fig. S6A), as previously described,⁵⁰ and the data showed that infants with HB ($85\text{--}425 \mu\text{mol/L}$ total bilirubin) displayed significantly lower ILC2 levels than those in healthy control infants, infants recovered from jaundice, and adult controls (Fig. 7a). Moreover, infants with severe HB (total serum bilirubin higher than $221 \mu\text{mol/L}$)^{23,51} displayed lower ILC2 levels than those in infants with mild HB (Fig. 7b). However, no noticeable differences were found in the

levels of ILC1s or ILC3s among different groups (Supplementary Fig. S6B). Further linear regression analysis revealed a significant correlation between the frequencies of ILC2s, but not ILC1s or ILC3s, and total bilirubin or UCB in the peripheral blood of infants (Fig. 7c and Supplementary Figs. S6C and S6D). Meanwhile, no correlations were found between ILC2s and other clinical parameters, including gestational age, birth weight, and the way of delivery (Supplementary Fig. S6E). In addition to the decreased levels, ILC2s from infants with severe HB displayed impaired function, as indicated by their reduced ability to produce effector cytokines (Fig. 7d). Consistently, the levels of p-ERK1/2 (Fig. 7e)

and GATA3 (Fig. 7f) in ILC2s from newborns with HB were dramatically lower than those in ILC2s from healthy controls. Collectively, these observations indicate that bilirubin may play a protective role against airway inflammation in newborns by suppressing ILC2s.

DISCUSSION

Human neonates develop HB physiologically.⁵¹ However, the beneficial effects of bilirubin on infant health are not fully understood. Herein, we demonstrated that bilirubin exerted suppressive effects on ILC2 responses, thereby contributing to the prevention of allergic inflammation in infants. Considering the allergen-induced challenge and the type 2 immunity-biased feature of newborns,⁵² this study supports the notion that HB may represent a protective mechanism for human beings after birth.

The beneficial effects of bilirubin against allergic inflammation have long been appreciated in adults.^{53,54} Patients with jaundice showed spontaneous remission of immunologic diseases, including allergy⁵⁴ and asthma.⁵³ Kim et al.¹⁹ showed that bilirubin inhibited Th2 responses both in vivo and in vitro. Other studies have reported that bilirubin levels at the higher end of the normal range were associated with a lower risk of respiratory disease, suggesting a protective role of bilirubin in the lungs.^{55,56} However, conflicting observations have also been reported. Several studies have shown that neonatal jaundice increases the rate and severity of childhood asthma in subjects aged up to 7–10 years old and may be a risk factor for childhood asthma.^{22,57} Therefore, the clinical value of bilirubin in allergic inflammation in different populations warrants further investigation. In this study, a significant induction of bilirubin metabolism in the lungs was observed in ILC2-driven airway inflammation models, and blocking bilirubin production aggravated airway inflammation. These findings indicate that allergen exposure could induce bilirubin synthesis, which in turn suppresses airway inflammation during type 2 innate immune responses in the lungs. The negative correlation between ILC2s and bilirubin in infants further supports this possibility.

Although high concentrations of UCB are potentially injurious to the basal ganglia and neurons,⁵⁸ studies have indicated that at physiological concentrations, this metabolite has anti-inflammatory effects under a variety of conditions, such as experimental autoimmune encephalomyelitis (EAE)²⁰ and dextran sodium sulfate (DSS)-induced murine colitis.^{34,59} More recently, bilirubin has been shown to bind to the peroxisome proliferator activated receptor- α (PPAR α), and this interaction may be the key to the protective metabolic functions of bilirubin.⁶⁰ Other studies have demonstrated the protective effects of HB in preventing the development of chronic liver disease,⁶¹ diabetes,⁶² and obesity.⁶³ The biological function of ILC2s in tissues other than lungs has been well documented,⁶⁴ and the administration of bilirubin has been shown to suppresses the systemic response of ILC2s to the IL-33 challenge, including in the mLN, liver, and adipose tissues. Therefore, the biological significance of bilirubin-mediated ILC2 suppression in other tissues deserves further investigation, which could provide an insight into its effects on other diseases.

Nevertheless, several issues remain to be addressed. First, our preliminary results clearly showed the induction of bilirubin-metabolizing enzymes in lung epithelial cells, rather than in immune cells. However, the source of bilirubin in the lungs, as well as the molecular events causing the induction of bilirubin-related genes after allergen exposure, still remains to be determined. Second, it is unclear how bilirubin, after it is generated in the lung, affects ERK signaling in ILC2s. UCB accounts for more than 95% of total serum bilirubin in healthy adults.⁶⁵ It is selectively taken up by hepatocytes, conjugated to glucuronic acid by UGT1A1, and then secreted into bile across the canalicular membrane.⁶⁶ As

bilirubin is hydrophobic in nature and has high permeability through lipid bilayer membranes, UCB has been suggested to cross cellular membranes by diffusion and can be intimately attached to cell membranes.^{67,68} Its direct interaction with cell membranes or cell entry by passive diffusion are possible mechanisms by which UCB elicits intracellular signaling. Third, studies on the protective effects of bilirubin against inflammatory diseases, including colitis,³⁴ EAE,²⁰ and pneumonia,¹⁹ have been limited to animal models to date. More animal studies and preclinical trials of bilirubin are needed before its protective effect can be applied to clinical treatment. In addition, although the effects of bilirubin on the activity of intracellular kinases are well documented,^{41,42} the detailed mechanism of bilirubin involvement in ERK phosphorylation in ILC2s warrants further investigation.

In summary, our study revealed that the inducible production of endogenous bilirubin represented a novel mechanism of ILC2 suppression, which might have therapeutic value in protecting infants from allergic airway inflammation.

METHODS

Animals

Rag-1^{-/-} mice (B6.129S7-Rag1^{tm1Mom}/JNju) and NCG mice (NOD-Prkdc^{em26Cd52}Il2rg^{em26Cd22}/Nju) were purchased from Nanjing Biomedical Research Institute, China. C57BL/6J mice were purchased from Guangdong Medical Laboratory Animal Center, China. All mice were maintained in specific pathogen-free condition room and 7–8 weeks old female mice were used for experiments. Littermates of the same sex were randomly assigned to experimental groups. During housing, animals were monitored twice daily for health status. No adverse events were observed. In order to minimize potential confounders, each batch of experimental model was completed by the same person and each experiment was repeated at least twice. The experimenters were blinded to the group allocation while processing data. All animal experimental procedures were approved by the IACUC of Tianjin Medical University (Tianjin, China) and Sun Yat-sen University (Guangzhou, China).

Human samples

This study included a series of infants administrated into the Third Affiliated Hospital of Sun Yat-sen University, Guangzhou, China from July 2017 to August 2020. A total of 91 infants (0–10 days old) were included. The peripheral blood samples were taken from infants at the summit of jaundice which were considered to be hyperbilirubinemia when serum total bilirubin was 85–425 $\mu\text{mol/L}$ ($n = 50$), infants who had recovered from hyperbilirubinemia had serum total bilirubin concentration <85 $\mu\text{mol/L}$ ($n = 10$), and 31 healthy infant donors and 19 healthy adult donors were collected as control.

Asthma patients (age 6–11 years) from Guangzhou Women and Children's Medical Center, Guangzhou, China, were recruited in this study. Inclusion criteria for allergic asthma was performed by Severe Asthma Research Program⁶⁹ and the Global Initiative for Asthma (GINA) Program. Patients with mild asthma had positive skin prick test responses, FEV1 of 70% of predicted value or greater, and used less inhaled corticosteroids (<210 $\mu\text{g/d}$) with no use of inhaled β_2 -agonists and Leukotriene antagonists. Severe asthmatic patients had: (1) prebronchodilator FEV1 of less than 60% of predicted value; (2) use of inhaled corticosteroids (>400 $\mu\text{g/d}$); (3) frequent use of inhaled β_2 -agonists and Leukotriene antagonists. Healthy donors with similar ages were used as control. Baseline characteristics are summarized in Supplementary Table S1 in this article's supplementary material.

For collection of human cord blood samples, placental cord blood was collected from women during delivery in Guangzhou Women and Children's Medical Center, Guangzhou, China. Women with acute infections (including pneumonia and urinary tract infections) or fever were excluded. All subjects were screened for antibodies against serum HIV-1, hepatitis B surface antigen (HBsAg), antibodies against hepatitis C virus (HCV), hepatitis D virus (HDV) antigen, and HDV. Individuals with positive results were excluded.

For experiments using human samples, written informed consent was received from the participants or their legal guardians, and the protocol was approved by the human ethics committees of Sun Yat-sen University

(Guangzhou, China) and Guangzhou Women and Children's Medical Center (Guangzhou, China).

Bilirubin treatment in vivo

C57BL/6J mice were intraperitoneally injected with unconjugated bilirubin (UCB, Sigma-Aldrich, USA) (25 mg/kg) dissolved in an aqueous solution containing 2 M NaOH and 200 mM Tris-HCl (pH 8.4), and adjusted with 0.5 M HCl to pH 7.0. To deplete the endogenous bilirubin, 1,4-bis-[2-(3,5-dichloropyridyloxy)] benzene (TCPOBOP, 3 mg/kg/mouse, MEMD Millipore Corp., USA) and zinc protoporphyrin IX (ZNPP, 25 mg/kg/mouse, Frontier Scientific, USA) were used.

IL-33 administration

Mice were intraperitoneally injected with 500 ng IL-33 (BioLegend) on days 0, 1, 2 and 3 as described.²⁵ Mice were sacrificed 24 h after the last injection, lungs were harvested and analyzed. Alternatively, mice were intranasal instillation of 500 ng IL-33 on days 0, 1 and 2.³ Mice were sacrificed on day 3, and the BAL fluid and lungs were collected and analyzed.

Mouse models of allergic airway inflammation

For induction of papain-induced acute type 2 airway inflammation,²⁶ 7–8 weeks old mice were anesthetized, followed by intranasal (*i.n.*) administration with papain (20 µg papain in 40 µl PBS, daily, Sigma-Aldrich) or PBS for 5 consecutive days. The BAL fluid and lungs were collected for analysis on day 6. For *Alternaria alternata*-induced airway inflammation, 7–8 weeks old mice were anesthetized and intranasally administrated with 100 µg *Alternaria alternata* (AA, Greerlabs, Lenoir, NC) in 40 µl PBS for 4 consecutive days as previously described.³ Mice were sacrificed 24 h after the last challenge. The BAL fluid and lungs were collected and analyzed. For OVA-induced chronic allergic inflammation,²⁵ 7–8 weeks old mice were *i.p.* sensitized with 100 µg OVA (Grade V, emulsified in 10 mg of aluminum hydroxide, Sigma-Aldrich) on days 0 and 7, followed by intranasal instillation with OVA (100 µg in 40 µl PBS) on days 14, 15, 16, and 17. Mice were sacrificed for analysis 24 h after the last challenge.

Measurement of bilirubin

The concentrations of serum bilirubin in mice or asthma patients were measured by total and direct bilirubin kits from Sigma-Aldrich. The measurement of human serum bilirubin and red blood cell counts was performed by Sysmex XN9000 automatic modular blood humoral analyzer (Sysmex Corporation, Japan).

Flow cytometric analysis and sorting

Single-cell suspensions were blocked with anti-Fc receptor antibody (anti-CD16/CD32) before staining with fluorochrome-conjugated antibodies. Antibodies used are listed in Supplementary Table S2. Dead cells were excluded by a cell viability dye (Live/dead fixable Viability Dye, Invitrogen) for subsequent analysis. For the flow cytometric sorting, a BD FACSAriaIII (BD Bioscience) was used. To sort mouse ILC2s, cells were first depleted of T cells, B cells, NK cells and myeloid, and erythroid lineages by labeling with biotin-conjugated lineage antibodies cocktail containing anti-CD3e, anti-CD45R/B220, anti-CD11b, anti-Ly6G, anti-Erythroid marker (TER-119), anti-CD11c, anti-NK1.1, anti-CD4, anti-CD5, anti-CD8a, anti-TCRβ, anti-TCRγδ, followed by streptavidin-paramagnetic particles (BD Bioscience, USA) according to manufacturer's instructions. The collected cells were then stained with fluorochrome-conjugated antibodies, including anti-CD45, anti-CD90.2, anti-CD25, and anti-ST2 before sorting. For human ILC2 sorting, PBMCs were labeled with biotin-conjugated anti-CD2, anti-CD3, anti-CD14, anti-CD16, anti-CD19, anti-CD56, anti-CD235a, anti-TCRαβ, anti-TCRγδ, anti-FCεR1a, anti-CD94, and anti-CD11C. Then, magnetic beads were used to deplete T cells, B cells, NK cells, myeloid cells, granulocytes, and red blood cells. The acquired lineage negative cells were stained with indicated fluorochrome-conjugated antibodies for ILC2s (CD45⁺CD127⁺CRTH2⁺). All the cells were sorted with a purity ≥95%. For intracellular cytokine staining, lung leukocytes were stimulated with PMA (50 ng/mL, Sigma-Aldrich), Ionomycin (1 µg/mL, Sigma) and Brefeldin A (1 µg/mL, Thermo Fisher Scientific) for 4 h at 37 °C, then stained for ILC2 markers, followed by IC Fixation Buffer (Thermo Fisher Scientific) and stained with anti-IL-13 and anti-IL-5 antibodies.

Adoptive transfer of ILC2

Lung ILC2s (3 × 10⁴ cells/mouse) were sorted from IL-33 challenged C57BL/6J mice, followed by tail intravenous injection into NCG mice. Mice were then

challenged with IL-33 (*i.n.*) for 3 consecutive days to induce lung inflammation. Mice were sacrificed and analyzed 24 h after the last challenge.

In vitro culture of ILC2

For ILC2 function analysis in vitro, lung ILC2s were cultured in 96-well round-bottom plates with a density of 5 × 10³ per well, treated with the vehicle or UCB (Sigma-Aldrich, USA, 50 µM) and /or Honokiol (MedChem-Express, 5 µM) and /or Bisindolylmaleimide I (BIM I, MedChemExpress, 5 µM) in the presence of mouse IL-33 (20 ng/ml), IL-2 (10 ng/ml) and IL-7 (20 ng/ml) for 72 h. Then, the amount of cytokines in culture supernatants was measured by ELISA. To evaluate human ILC2 function, human ILC2s (5000 cells/well) were cultured in 96-well round-bottom plates in the presence of recombinant human IL-33 (20 ng/ml), IL-7 (20 ng/ml) and IL-2 (20 ng/ml) for 3 days and the supernatants were collected for cytokines measurement.

qRT-PCR

Total RNA from indicated cells was extracted by using TRIzol (Invitrogen) and reverse transcribed with a synthesis kit (Takara, Japan). Gene mRNA expression was analyzed by qPCR with SYBR green chemistry (Takara, Japan). The sequences of primer used were listed in Supplementary Table S3.

Enzyme-linked immunosorbent assay (ELISA)

The BAL fluid from mice or the supernatants from cultured ILC2 were collected. The levels of individual cytokines were determined by ELISA, following the manufacturer's instructions (eBioscience, USA).

Citrobacter rodentium model

Mice were orally gaged with 200 µl of PBS containing 1 × 10⁹ colony-forming units (CFUs) of *Citrobacter rodentium*. 24 h after infection, mice were injected with bilirubin (*i.p.* 25 mg/kg) daily. Body weights were monitored daily. Mice were sacrificed on day 7, and colon length were measured and flow cytometric analysis of ILC1 and ILC3 were performed. *Citrobacter rodentium* were kindly provided by Dr. Ju Qiu from Shanghai Institutes for Biological Sciences, Chinese Academy of Sciences.

Retroviral infection of ILC2

We followed the procedures described previously.⁷⁰ Sorted lung ILC2s were cultured overnight in the presence of 10 ng/ml IL-2, IL-7, and IL-33, followed by treatment with retrovirus-containing supernatants supplemented with polybrene (8 µg/ml). Cells were then centrifuged at 1000 × *g* for 2 h at 32 °C, and cultured at 37 °C for another 6 h. Cells were subsequently washed with 1640 medium and cultured in fresh complete medium containing 10 ng/ml of IL-2, IL-7, and IL-33 in the presence of vehicle or UCB (50 µM). Four days later, the supernatants were collected for analysis of IL-5 and IL-13 content by ELISA.

Lung histology

Lung tissues were fixed in 4% phosphate-buffered formaldehyde solution for 24 h. Tissue sections were prepared and stained with hematoxylin-eosin (H&E) to assess inflammation. Inflammation was determined by semi-quantitative scoring (0–4: 0, none; 1, mild; 2, moderate; 3, marked; and 4, severe). An increment of 0.5 was used when the inflammation fell between two levels. Three fields were selected randomly for scoring using a Leica microscope by two treatment-blind pathologists independently. Immunohistochemistry were performed following the established protocols.⁷¹ Mouse anti-bilirubin mAb was purchased from Abbeva, UK.

Statistical analysis

All data are derived from two to four independent experiments. Data are shown as means ± SEM except for Supplementary Table 1 shown as means ± SD and statistical significance was determined by two-tailed unpaired Student's *t* test or one-way ANOVA with Bonferroni post-test. Correlations between different parameters were analyzed using a Spearman's rank correlation test. Statistical analysis was performed with GraphPad Prism 6.0 software (Graphpad Software, La Jolla, CA). *P* < 0.05 was considered significant.

DATA AVAILABILITY

Further information and requests for resources and data in this study are available from the corresponding author (J.Z., zhoujie@tmu.edu.cn) without restriction.

REFERENCES

1. Dahlgren, M. W. & Molofsky, A. B. All along the watchtower: group 2 innate lymphoid cells in allergic responses. *Curr. Opin. Immunol.* **54**, 13–19 (2018).
2. Vivier, E. et al. Innate lymphoid cells: 10 years on. *Cell* **174**, 1054–1066 (2018).
3. Maazi, H. et al. ICOS:ICOS-ligand interaction is required for type 2 innate lymphoid cell function, homeostasis, and induction of airway hyperreactivity. *Immunity* **42**, 538–551 (2015).
4. Wojno, E. D. T. & Artis, D. Emerging concepts and future challenges in innate lymphoid cell biology. *J. Exp. Med.* **213**, 2229–2248 (2016).
5. Eberl, G., Colonna, M., Di Santo, J. P. & McKenzie, A. N. Innate lymphoid cells. Innate lymphoid cells: a new paradigm in immunology. *Science* **348**, aaa6566 (2015).
6. Bartemes, K. R., Kephart, G. M., Fox, S. J. & Kita, H. Enhanced innate type 2 immune response in peripheral blood from patients with asthma. *J. Allergy Clin. Immunol.* **134**, 671–678 (2014).
7. Liu, T. et al. Type 2 innate lymphoid cells: a novel biomarker of eosinophilic airway inflammation in patients with mild to moderate asthma. *Respir. Med.* **109**, 1391–1396 (2015).
8. Monticelli, L. A., Sonnenberg, G. F. & Artis, D. Innate lymphoid cells: critical regulators of allergic inflammation and tissue repair in the lung. *Curr. Opin. Immunol.* **24**, 284–289 (2012).
9. Klose, C. S. & Artis, D. Innate lymphoid cells as regulators of immunity, inflammation and tissue homeostasis. *Nat. Immunol.* **17**, 765–774 (2016).
10. Doherty, T. A. et al. Lung type 2 innate lymphoid cells express cysteinyl leukotriene receptor 1, which regulates TH2 cytokine production. *J. Allergy Clin. Immunol.* **132**, 205–213 (2013).
11. Kabata, H., Moro, K. & Koyasu, S. The group 2 innate lymphoid cell (ILC2) regulatory network and its underlying mechanisms. *Immunological Rev.* **286**, 37–52 (2018).
12. Wilhelm, C. et al. Critical role of fatty acid metabolism in ILC2-mediated barrier protection during malnutrition and helminth infection. *J. Exp. Med.* **213**, 1409–1418 (2016).
13. Wojno, E. D. et al. The prostaglandin D(2) receptor CRTH2 regulates accumulation of group 2 innate lymphoid cells in the inflamed lung. *Mucosal Immunol.* **8**, 1313–1323 (2015).
14. Jangi, S., Otterbein, L. & Robson, S. The molecular basis for the immunomodulatory activities of unconjugated bilirubin. *Int. J. Biochem. Cell Biol.* **45**, 2843–2851 (2013).
15. Stocker, R., Yamamoto, Y., McDonagh, A. F., Glazer, A. N. & Ames, B. N. Bilirubin is an antioxidant of possible physiological importance. *Science* **235**, 1043–1046 (1987).
16. Bonelli, M. et al. Heme oxygenase-1 end-products carbon monoxide and biliverdin ameliorate murine collagen induced arthritis. *Clin. Exp. Rheumatol.* **30**, 73–78 (2012).
17. Keshavan, P. et al. Unconjugated bilirubin inhibits VCAM-1-mediated transendothelial leukocyte migration. *J. Immunol.* **174**, 3709–3718 (2005).
18. Kitada, O. et al. Heme oxygenase-1 (HO-1) protein induction in a mouse model of asthma. *Clin. Exp. Allergy.* **31**, 1470–1477 (2001).
19. Kim, D. E. et al. Bilirubin nanoparticles ameliorate allergic lung inflammation in a mouse model of asthma. *Biomaterials* **140**, 37–44 (2017).
20. Liu, Y. et al. Bilirubin possesses powerful immunomodulatory activity and suppresses experimental autoimmune encephalomyelitis. *J. Immunol.* **181**, 1887–1897 (2008).
21. Das, R. R. & Naik, S. S. Neonatal hyperbilirubinemia and childhood allergic diseases: a systematic review. *Pediatr. Allergy Immunol.* **26**, 2–11 (2015).
22. Huang, L. et al. Neonatal bilirubin levels and childhood asthma in the US Collaborative Perinatal Project, 1959–1965. *Am. J. Epidemiol.* **178**, 1691–1697 (2013).
23. Dennery, P. A., Seidman, D. S. & Stevenson, D. K. Neonatal hyperbilirubinemia. *N. Engl. J. Med.* **344**, 581–590 (2001).
24. Ostrow, J. D., Pascolo, L., Shapiro, S. M. & Tiribelli, C. New concepts in bilirubin encephalopathy. *Eur. J. Clin. Invest.* **33**, 988–997 (2003).
25. Lei, A. H. et al. ICAM-1 controls development and function of ILC2. *J. Exp. Med.* **215**, 2157–2174 (2018).
26. Monticelli, L. A. et al. Arginase 1 is an innate lymphoid-cell-intrinsic metabolic checkpoint controlling type 2 inflammation. *Nat. Immunol.* **17**, 656–665 (2016).
27. Li, Q. et al. E3 ligase VHL promotes group 2 innate lymphoid cell maturation and function via glycolysis inhibition and induction of interleukin-33 receptor. *Immunity* **48**, 258–270 e255 (2018).
28. Neumann, K. et al. A proinflammatory role of type 2 innate lymphoid cells in murine immune-mediated hepatitis. *J. Immunol.* **198**, 128–137 (2017).
29. Brestoff, J. R. et al. Group 2 innate lymphoid cells promote beiging of white adipose tissue and limit obesity. *Nature* **519**, 242–246 (2015).
30. Karta, M. R. et al. beta(2) integrins rather than beta(1) integrins mediate Alternaria-induced group 2 innate lymphoid cell trafficking to the lung. *J. Allergy Clin. Immunol.* **141**, 329–338 (2018).
31. Doherty, T. A. & Broide, D. H. Group 2 innate lymphoid cells: new players in human allergic diseases. *J. Invest. Allergol. Clin. Immunol.* **25**, 1–11 (2015).
32. Hirose, K., Iwata, A., Tamachi, T. & Nakajima, H. Allergic airway inflammation: key players beyond the Th2 cell pathway. *Immunol. Rev.* **278**, 145–161 (2017).
33. Halim, T. Y. F. et al. Tissue-restricted adaptive type 2 immunity is orchestrated by expression of the costimulatory molecule OX40L on group 2 innate lymphoid cells. *Immunity* **48**, 1195–1207 (2018).
34. Longhi, M. S. et al. Bilirubin suppresses Th17 immunity in colitis by upregulating CD39. *JCI Insight* **2**, e92791 (2017).
35. Lee, Y. et al. Hyaluronic acid-bilirubin nanomedicine for targeted modulation of dysregulated intestinal barrier, microbiome and immune responses in colitis. *Nat. Mater.* **19**, 118–126 (2020).
36. Bao, L. et al. Role of heme Oxygenase-1 in low dose radioadaptive response. *Redox Biol.* **8**, 333–340 (2016).
37. Kirkby, K. A. & Adin, C. A. Products of heme oxygenase and their potential therapeutic applications. *Am. J. Physiol. Ren. Physiol.* **290**, F563–F571 (2006).
38. Huang, W. et al. Induction of bilirubin clearance by the constitutive androstane receptor (CAR). *Proc. Natl Acad. Sci. USA* **100**, 4156–4161 (2003).
39. Hoyler, T. et al. The transcription factor GATA-3 controls cell fate and maintenance of type 2 innate lymphoid cells. *Immunity* **37**, 634–648 (2012).
40. Yagi, R. J. et al. The transcription factor GATA3 is critical for the development of all IL-7R alpha-expressing innate lymphoid cells. *Immunity* **40**, 378–388 (2014).
41. Hansen, T. W. R., Mathiesen, S. B. W. & Walaas, S. I. Bilirubin has widespread inhibitory effects on protein phosphorylation. *Pediatr. Res.* **39**, 1072 (1996).
42. Taille, C. et al. Heme oxygenase inhibits human airway smooth muscle proliferation via a bilirubin-dependent modulation of ERK1/2 phosphorylation. *J. Biol. Chem.* **278**, 27160–27168 (2003).
43. Yamashita, M. et al. Ras-ERK MAPK cascade regulates GATA3 stability and Th2 differentiation through ubiquitin-proteasome pathway. *J. Biol. Chem.* **280**, 29409–29419 (2005).
44. Suzuki, M., Morita, R., Hirata, Y., Shichita, T. & Yoshimura, A. Spred1, a suppressor of the Ras-ERK pathway, negatively regulates expansion and function of group 2 innate lymphoid cells. *J. Immunol.* **195**, 1273–1281 (2015).
45. Lin, Z. et al. JUNB-FBXO21-ERK axis promotes cartilage degeneration in osteoarthritis by inhibiting autophagy. *Aging Cell* **20**, e13306 (2021).
46. Puente, L. G., He, J. S. & Ostergaard, H. L. A novel PKC regulates ERK activation and degranulation of cytotoxic T lymphocytes: Plasticity in PKC regulation of ERK. *Eur. J. Immunol.* **36**, 1009–1018 (2006).
47. Tsao, H. K., Chiu, P. H. & Sun, S. H. PKC-dependent ERK phosphorylation is essential for P2X7 receptor-mediated neuronal differentiation of neural progenitor cells. *Cell Death Dis.* **4**, e751 (2013).
48. Madoufi, F. et al. Protein kinase C theta controls type 2 innate lymphoid cell and TH2 responses to house dust mite allergen. *J. Allergy Clin. Immunol.* **139**, 1650–1666 (2017).
49. Gloria-Bottini, F. & Bottini, E. Is there a role of early neonatal events in susceptibility to allergy? *Int. J. Biomed. Sci.* **6**, 8–12 (2010).
50. Vely, F. et al. Evidence of innate lymphoid cell redundancy in humans. *Nat. Immunol.* **17**, 1291–1299 (2016).
51. Fujiwara, R. et al. Systemic regulation of bilirubin homeostasis: Potential benefits of hyperbilirubinemia. *Hepatology* **67**, 1609–1619 (2018).
52. Levy, O. Innate immunity of the newborn: basic mechanisms and clinical correlates. *Nat. Rev. Immunol.* **7**, 379–390 (2007).
53. Ohrui, T., Yasuda, H., Yamaya, M., Matsui, T. & Sasaki, H. Transient relief of asthma symptoms during jaundice: a possible beneficial role of bilirubin. *Tohoku J. Exp. Med* **199**, 193–196 (2003).
54. Gorin, N. Temporary relief of asthma by jaundice; report of three cases. *J. Am. Med. Assoc.* **141**, 24 (1949).
55. Horsfall, L. J. et al. Serum bilirubin and risk of respiratory disease and death. *JAMA* **305**, 691–697 (2011).
56. Leem A. Y. et al. Association of serum bilirubin level with lung function decline: a Korean community-based cohort study. *Respir. Res.* **19**, 99 (2018).
57. Ku, M. S. et al. Neonatal jaundice is a risk factor for childhood asthma: a retrospective cohort study. *Pediatr. Allergy Immunol.* **23**, 623–628 (2012).
58. Brites, D. The evolving landscape of neurotoxicity by unconjugated bilirubin: role of glial cells and inflammation. *Front. Pharm.* **3**, 88 (2012).
59. Zucker, S. D. et al. Bilirubin prevents acute DSS-induced colitis by inhibiting leukocyte infiltration and suppressing upregulation of inducible nitric oxide synthase. *Am. J. Physiol. Gastrointest. Liver Physiol.* **309**, G841–G854 (2015).
60. Stec D. E. et al. Bilirubin Binding to PPAR alpha Inhibits Lipid Accumulation. *Plos One* **2016**; **11**, e0153427.
61. Kwak, M. S. et al. Serum bilirubin levels are inversely associated with nonalcoholic fatty liver disease. *Clin. Mol. Hepatol.* **18**, 383–390 (2012).
62. Vitek, L. The role of bilirubin in diabetes, metabolic syndrome, and cardiovascular diseases. *Front Pharm.* **3**, 55 (2012).

63. Hinds, T. D. et al. Increased HO-1 levels ameliorate fatty liver development through a reduction of heme and recruitment of FGF21. *Obesity* **22**, 705–712 (2014).
64. Gasteiger, G., Fan, X., Dikiy, S., Lee, S. Y. & Rudensky, A. Y. Tissue residency of innate lymphoid cells in lymphoid and nonlymphoid organs. *Science* **350**, 981–985 (2015).
65. Muraca, M. & Blanckaert, N. Liquid-chromatographic assay and identification of mono- and diester conjugates of bilirubin in normal serum. *Clin. Chem.* **29**, 1767–1771 (1983).
66. Erlinger, S., Arias, I. M. & Dhumeaux, D. Inherited disorders of bilirubin transport and conjugation: new insights into molecular mechanisms and consequences. *Gastroenterology* **146**, 1625–1638 (2014).
67. Baranano, D. E., Rao, M., Ferris, C. D. & Snyder, S. H. Biliverdin reductase: a major physiologic cytoprotectant. *Proc. Natl Acad. Sci. USA* **99**, 16093–16098 (2002).
68. Zucker, S. D., Goessling, W. & Hoppin, A. G. Unconjugated bilirubin exhibits spontaneous diffusion through model lipid bilayers and native hepatocyte membranes. *J. Biol. Chem.* **274**, 10852–10862 (1999).
69. Fitzpatrick, A. M. et al. Heterogeneity of severe asthma in childhood: confirmation by cluster analysis of children in the National Institutes of Health/National Heart, Lung, and Blood Institute Severe Asthma Research Program. *J. Allergy Clin. Immunol.* **127**, 382–389 e381–313 (2011).
70. Yang, Q. et al. T cell factor 1 is required for group 2 innate lymphoid cell generation. *Immunity* **38**, 694–704 (2013).
71. Gueders, M. M. et al. Matrix metalloproteinase-8 deficiency promotes granulocytic allergen-induced airway inflammation. *J. Immunol.* **175**, 2589–2597 (2005).

ACKNOWLEDGEMENTS

This work was supported by the following grants to J.Z: National Natural Science Foundation of China (Nos. 81925018, 81771665), Start-up Fund for High-level Talents of Tianjin Medical University, Key Project of Tianjin Natural Science Foundation

(2-
0J-
C-

ZDJC00670). This work was also supported by grants to J.H: National Natural Science Foundation of China (82001691) and China Postdoctoral Science Foundation (2020M672582).

AUTHOR CONTRIBUTIONS

J.H., G.J. and X.L. performed the experiments, analyzed the data, participated in figure organization and manuscript writing; Q.X., Y.C., A.L., P.Z. and Q.Y. participated in mouse breeding and mouse model construction; H.X. and G.L. participated in experiments; X.L., K.S. and M.Z. participated in the experiments related to clinical samples; Z.Y. provided suggestions for experimental design and supervised the project; J.Z. conceptualized, supervised, interpreted the experiments and wrote the manuscript.

COMPETING INTERESTS

The authors declare no competing interests.

ADDITIONAL INFORMATION

Supplementary information The online version contains supplementary material available at <https://doi.org/10.1038/s41385-021-00460-0>.

Correspondence and requests for materials should be addressed to Zhi Yao or Jie Zhou.

Reprints and permission information is available at <http://www.nature.com/reprints>

Publisher's note Springer Nature remains neutral with regard to jurisdictional claims in published maps and institutional affiliations.